DOI: 10.1002/chem.200800600

On the Mechanism of d–f Energy Transfer in Ru^{II}/Ln^{III} and Os^{II}/Ln^{III} Dyads: Dexter-Type Energy Transfer Over a Distance of 20 Å

Theodore Lazarides,[a] Daniel Sykes,[b] Stephen Faulkner,[b] Andrea Barbieri,[c] and Michael D. Ward*[a]

Abstract: We have used time-resolved luminescence methods to study rates of photoinduced energy transfer (PEnT) from $[M(bipy)_3]^{2+}$ (M = Ru, Os) chromophores to Ln^{III} ions with low-energy f–f states (Ln = Yb, Nd, Er) in d–f dyads in which the metal fragments are separated by a saturated $-CH_2CH_2-$ spacer, a *p*-C_6H_4 spacer, or a *p*-$(C_6H_4)_2$ spacer. The finding that d→f PEnT is much faster across a conjugated *p*-C_6H_4 spacer than it is across a shorter CH_2CH_2 spacer points unequivocally to a Dexter-type energy transfer, involving electronic coupling mediated by the bridging ligand orbitals (superexchange) as the dominant mechanism. Comparison of the distance dependence of the Ru→Nd energy-transfer rate across different conjugated spacers [*p*-C_6H_4 or *p*-$(C_6H_4)_2$ groups] is also consistent with this mechanism. Observation of Ru→Nd PEnT (as demonstrated by partial quenching of the Ru^{II}-based ^{3}MLCT emission (MLCT = metal-to-ligand charge transfer), and the growth of sensitised Nd^{III}-based emission at 1050 nm) over approximately 20 Å by an exchange mechanism is a departure from the normal situation with lanthanides, in which long-range energy transfer often involves through-space Coulombic mechanisms.

Keywords: bridging ligands · energy transfer · lanthanides · luminescence · osmium · ruthenium

Introduction

The use of d-block chromophores as antenna groups to generate sensitised luminescence from Ln^{III} centres (Ln = a lanthanide), following d→f energy transfer, is an area that has attracted much attention in the last few years.[1] Many types of transition metal unit have been employed in d–f hybrid complexes in this way, because of their numerous desirable characteristics. These include strong absorbance of light in the visible region, a long-lived (usually ^{3}MLCT (MLCT = metal-to-ligand charge transfer)) excited state which can act as the energy donor, and a relatively low ^{3}MLCT energy (compared to organic chromophores) which is a good match for the f–f levels of Ln^{III} ions such as Pr^{III}, Nd^{III}, Er^{III} and Yb^{III} which generate near-infrared luminescence.[1]

There are two possible types of mechanism for sensitisation of lanthanide luminescence by energy transfer from a separate antenna unit (indeed, these apply in general to any energy transfer). The first is Dexter energy transfer, an electron exchange mechanism which requires orbital overlap between donor and acceptor components.[2] This is the mechanism typically assumed for sensitisation of lanthanide-based luminescence by directly coordinated ligands, through the ligand-based triplet excited state[2–4] (although there are a few exceptions, based on energy transfer from singlet excited states,[5] and mechanisms involving an electron-transfer step).[6] Because the Dexter mechanism requires direct donor–acceptor orbital overlap it is a short-range mechanism with an e^{-d} distance dependence (d = distance).[2] However in the case that donor and acceptor components are connected by conjugated bridging ligands, long-range donor–acceptor electronic coupling can occur through an indirect superexchange process mediated by the orbitals of the bridging ligand. Thus the double-electron exchange required for energy transfer by the Dexter mechanism can occur over substantial distances,[7,8] and this is still sometimes referred to loosely as "Dexter-type" energy transfer even though *direct* donor–acceptor orbital overlap is not in-

[a] Dr. T. Lazarides, Prof. M. D. Ward
Department of Chemistry, University of Sheffield
Sheffield S3 7HF (UK)
Fax: (+44) 114-222-9346
E-mail: m.d.ward@sheffield.ac.uk

[b] Dr. D. Sykes, Prof. S. Faulkner
Department of Chemistry, University of Manchester
Oxford Road, Manchester M13 9PL (UK)

[c] Dr. A. Barbieri
Istituto ISOF-CNR
Via P. Gobetti 101, 40129 Bologna (Italy)

volved. Like through-bond electron transfer, energy transfer by this mechanism also has an exponential decay with distance.[8,9]

The second energy-transfer mechanism arises from the Coulombic interaction between the donor and acceptor electric fields, and is a through-space interaction which is not dependent on orbital overlap between components. The simplest (dipole–dipole) component of this is the basis of Förster energy transfer,[10] which occurs best between donor and acceptor components in which the electronic transitions have substantial transition dipole moments. In the particular case of lanthanides as energy-acceptors the transition dipole moment of f–f transitions is small, and higher-order multipolar interactions can also be significant; in particular dipole–quadrupole interactions between the transition dipole moment of the donor, and the f–f transition, which may have a significant transition quadrupole moment.[7,11,12]

In the case of d–f hybrids, the d-block sensitiser unit is more remote from the Ln^{III} centre than a directly coordinated ligand would be, and there may be a lengthy bridging fragment (saturated or unsaturated) between energy donor and acceptor fragments.[1] The question therefore arises as to the mechanism of the energy-transfer process: is it a Coulombic through-space process (Förster-type,[10] but with a possible higher-order multipolar contribution[12]) or a through-bond electron-exchange process (Dexter-type,[2] but with the donor–acceptor electronic coupling provided by participation of bridging ligand orbitals in a superexchange process[8])?

In addition there are other factors to take into account in any consideration of energy-transfer mechanisms in d–f hybrids.

Firstly, there are specific selection rules for energy transfer to Ln^{III} ions,[13] based on changes in the angular momentum quantum number J: the restrictions are that $|\Delta J| = 0$, 1 for Dexter energy transfer (with the special case of $J = J' = 0$ being excluded) and $|\Delta J| = 2$, 4, 6 for multipolar Coulombic energy transfer, so in principle either mechanism may occur depending on which excited state of the Ln^{III} centre is involved and its $|\Delta J|$ value with respect to the ground state.

Secondly, the various processes are dependent on distance in a different way, with Förster (dipole–dipole) energy transfer depending on d^{-6}, and any higher-order dipole-quadrupole contribution to energy transfer varying as d^{-8}.[14] In contrast, Dexter energy-transfer (and its superexchange-mediated analogues) vary as e^{-d} because of their dependence on the electronic coupling (H).[9] Exchange-mediated energy transfer therefore decays with distance more rapidly than the Coulombic energy transfer. Thus, the very long range energy transfer involving luminescent Ln^{III} ions as donors in FRET-type biological assays (FRET = fluorescence resonance energy transfer) operates by the Coulombic mechanism.[15]

To investigate the issue of the energy-transfer mechanism over long distances in d–f dyads more closely, we have undertaken a systematic study of a series of related d–f dinuclear complexes based on the $[M(bipy)_3]^{2+}$ (bipy = 2,2′-bipyridine) derivatives shown in Scheme 1 (M = Ru, Os). These all contain a $[M(bipy)_3]^{2+}$ chromophore[16,17] connected to a vacant bipyridyl binding site by an organic spacer which is either saturated (complexes $Ru–CH_2CH_2$ and $Os–CH_2CH_2$, or unsaturated (complexes RuPh, OsPh and $RuPh_2$). Reaction of these with excess $[Ln(tta)_3(H_2O)_2]$ (tta = anion of thenyl-trifluoroacetone, see Scheme 2) in CH_2Cl_2 solution affords dinuclear d–f hybrids through an equilibrium reaction of the type shown in Scheme 2, in which the vacant bipyridyl site of the d-block "complex ligand" displaces two water ligands from the coordination sphere of the Ln^{III} species to give an eight-coordinate $[Ln(tta)_3(bipy)]$ centre.[18,19]

The Ln^{III} ions concerned are those which have low-energy luminescent excited states emitting in the near-IR region, and which can therefore be sensitised by the ^{3}MLCT states of the d-block chromophores. A combination of photophysical studies [measuring i) the degree of quenching of the Ru^{II} or Os^{II} energy-donors and ii) the occurrence of sensitised luminescence in the Ln^{III} energy-acceptors] and calculations

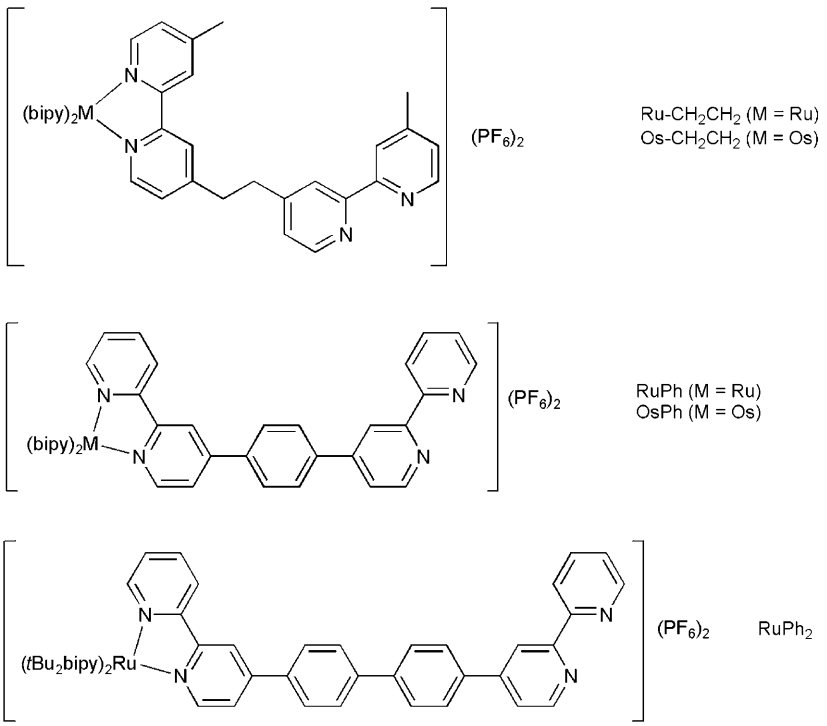

Scheme 1. The Ru^{II} and Os^{II} complexes used to prepare the d–f dyads.

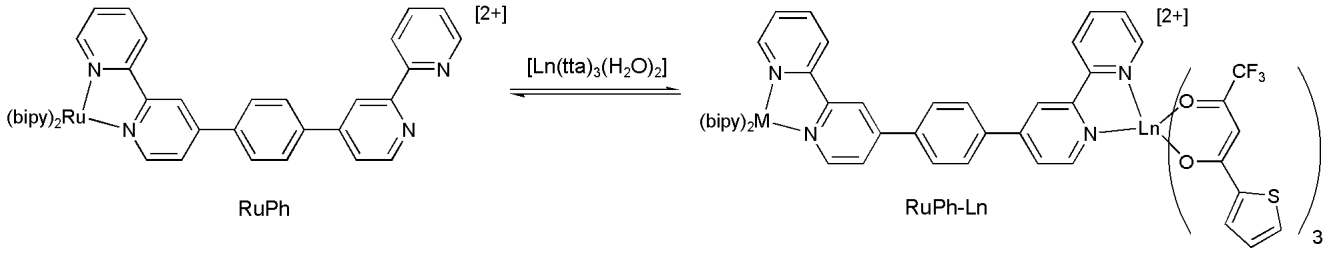

Scheme 2. Association of $Ln(tta)_3$ units to the vacant bipyridyl sites of the Ru^{II} and Os^{II} complexes.

unequivocally indicate that d→f energy transfer in the conjugated systems occurs completely through a bridging-ligand mediated exchange mechanism, and provides additional interesting information on the different abilities of Ru^{II} versus Os^{II} units to act as energy donors. A partial contribution to energy transfer by a Coulombic mechanism may be possible in the system with the saturated linker, where exchange energy transfer is disadvantaged by the reduced electronic coupling between the components.

We note that similar studies of energy transfer between two metal centres as a function of the bridging ligand (length, degree of saturation, rigidity etc.) have been carried out for many donor–acceptor dyads in which both components are based on transition metal (d-block) ions.[8,20] However such systematic studies have scarcely been performed for d–f dyads, a situation which is in part remedied by this work.

Results and Discussion

Choice of complexes: synthesis: The complexes (Scheme 1) were prepared and characterised by standard methods; some are known, and some are reported here for the first time (see the Experimental section for details). The set of complexes chosen allows for several comparisons of d→f energy-transfer rates in different systems, as follows:

i) Comparison of the effects of saturated versus unsaturated bridging ligands (Ru–CH_2CH_2/RuPh and Os–CH_2CH_2/OsPh) will indicate whether or not a conjugated pathway is necessary for energy transfer to occur (in which case an exchange mechanism for energy transfer will be operative), or whether it occurs just as easily across a saturated spacer (in which case the Coulombic energy-transfer mechanism will be operative).

ii) Comparison of related Ru/Os pairs (Ru–CH_2CH_2/Os-CH_2CH_2, and RuPh/OsPh) will allow the effectiveness of $[Ru(bipy)_3]^{2+}$ versus $[Os(bipy)_3]^{2+}$ as energy-donors to be evaluated; these complexes are ubiquitous as photosensitisers in polynuclear assemblies and have been of particular interest as sensitisers for Ln^{III}-based emisson in d–f dyads.[1]

iii) Comparison of the pair RuPh/$RuPh_2$ will allow the effect of increasing distance on energy transfer to be studied in a pair of complexes containing the same donor and acceptor groups.

iv) Finally, evaluation of the properties of d–f pairs based on a specific d-block unit but combined with different Ln^{III} ions, for example, RuPh with Nd^{III}, Er^{III} and Yb^{III} will allow investigation of the abilities of different Ln^{III} ions to act as energy acceptors according to their availability of f–f states.

Photophysical studies: *i) Properties of mononuclear Ru^{II} and Os^{II} complexes; formation of d–f dinuclear complexes in solution*: The UV/Vis spectra of the complexes show the usual intense π–π* transitions in the UV region and less intense MLCT absorptions in the visible region.[16,17] Characteristically, the Ru^{II} complexes show a ^{1}MLCT absorption manifold in which the maximum is at approximately 450 nm, whereas the Os^{II} complexes show both ^{1}MLCT absorptions ($\lambda < 500$ nm) and weaker, spin-forbidden ^{3}MLCT absorptions between 550 and 700 nm which are visible because of the higher spin-orbit coupling of Os^{II} compared with Ru^{II} ($\zeta_{Os} = 3{,}381\ cm^{-1}$, $\zeta_{Ru} = 1{,}042\ cm^{-1}$).[21] The spectra are summarised in Table 1 and two examples are shown in Figure 1.

Table 1. Absorption spectra of the complexes in CH_2Cl_2 at room temperature

Complex	λ_{max} [nm] ($10^{-3}\varepsilon$ [$M^{-1}cm^{-1}$])
Ru–CH_2CH_2	287 (90), 326 (≈9, sh), 358 (≈5, sh), 425 (≈10, sh), 456 (13)
RuPh	288 (93), 320 (≈35, sh), 360 (≈10, sh), 395 (≈8, sh), 430 (≈14, sh), 456 (18)
$RuPh_2$	288 (106), 334 (42), 435 (≈16, sh), 463 (20)
Os–CH_2CH_2	290 (92), 330 (9.7), 371 (10), 438 (12), 483 (13), 587 (3.4), 645 (2.9)
OsPh	290 (94), 325 (≈32, sh), 373 (14), 440 (17), 485 (17), 587 (4.8), 646 (4.4)

The luminescence properties of the mononuclear Ru^{II} and Os^{II} complexes are summarised in Table 2 and are typical of the well-known behaviour of Ru^{II} and Os^{II} bipyridyl complexes.[16,17] All three Ru^{II} complexes emit in aerated fluid solution in the region 600–630 nm, with lifetimes of hundreds of nanoseconds and quantum yields of 3–5 %. The two Os^{II} complexes show lower-energy luminescence with a maximum at approximately 720 nm, with lifetimes of <100 ns and quantum yields of approximately 1 %.

The effect of binding a $[Ln(tta)_3]$ unit at the secondary coordination site was then measured by titrating a solution of the relevant $[Ln(tta)_3(H_2O)_2]$ species into a solution of the

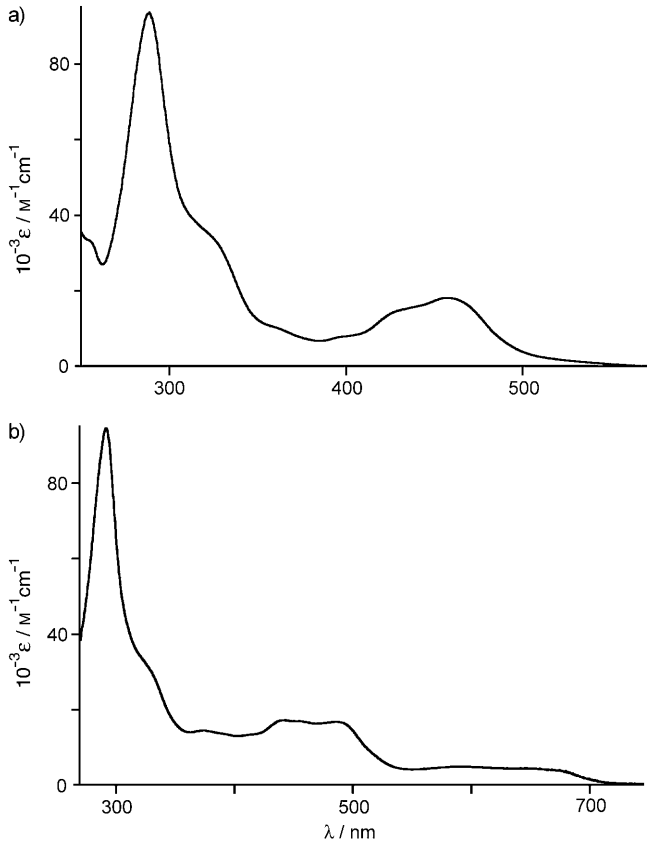

Figure 1. UV/Vis absorption spectra of a) RuPh and b) OsPh in CH_2Cl_2.

Table 2. Luminescence properties of the mononuclear Ru^{II} and Os^{II} complexes, and their dyad assemblies with Ln^{III} ions.

Compound	λ_{em} [nm][a]	$10^2\phi_{em}$[a]	$\lambda_{em}^{77\,K}$ [nm][b]	τ [ns][a]	τ_{Nd} [ns][a,c]	τ_{Yb} [ns][a,c]	τ_{Er} [ns][a,c]
Ru–CH_2CH_2	604	3.7	580	390	210	390	390
RuPh	603	4.3	580	520	48	250	190
$RuPh_2$	626	3.6	592	460	256	460	418
Os–CH_2CH_2	715	0.9	714	62	57	62	62
OsPh	720	1.4	717	80	51	76	76

[a] Measured in CH_2Cl_2 at room temperature. Estimated uncertainties: emission maxima, ±2 nm; quantum yields, ±20%; lifetimes, ±5%. [b] Measured in a EtOH/MeOH (4:1, v/v) frozen glass at 77 K. [c] Limiting value of the residual Ru^{II}- or Os^{II}-based emission at the end of the titration with the appropriate $[Ln(tta)_3(H_2O)_2]$, that is, in the Ru–Ln or Os–Ln adduct.

Ru^{II} or Os^{II} complex (typically 10^{-5} M in CH_2Cl_2), until no further change occurred in the Ru^{II}- or Os^{II}-based luminescence properties. Under these conditions the equilibrium in Scheme 2 lies substantially to the right: the magnitude of the association constant for the equilibrium in Scheme 2 is expected to be in the region 10^5–10^7 M^{-1},[1] and in agreement with this we found the Ru–Ln or Os–Ln dyad to be fully formed after addition of 5–10 equivalents of the appropriate $[Ln(tta)_3(H_2O)_2]$. All photophysical measurements on these mixtures were performed by using selective excitation of the Ru^{II}- or Os^{II}-based chromophore at 460 nm, a wavelength at which the $[Ln(tta)]_3$ units do not absorb so the excitation can be regarded as completely selective for the $[M(bipy)_3]^{2+}$ unit. Under these conditions the excess free (non-absorbing) $[Ln(tta)_3(H_2O)_2]$ species is "invisible" and does not contribute to the observed luminescence of the equilibrium mixture.

ii) Comparison of Ru–CH_2CH_2–Nd with RuPh–Nd: We will concentrate initially on the Ru^{II}–Nd^{III} systems. Nd^{III} has been demonstrated many times to be a particularly effective quencher of species which luminesce in the visible region, because it has a high density of f–f excited states between 11000 and 20000 cm^{-1}. The donor–acceptor spectroscopic overlap with d-block complexes which show visible-region luminescence is therefore higher than for other Ln^{III} ions.[1] In addition sensitised luminescence from Nd^{III} is easy to detect by the relatively intense emission band at approximately 1050 nm, a wavelength at which the residual luminescence from $[Ru(bipy)_3]^{2+}$-type luminophores has tailed off to zero and thus does not interfere.

The most striking contrast is between Ru–CH_2CH_2–Nd (see Scheme 2 for nomenclature) and RuPh–Nd, that is, between systems with saturated and conjugated bridges. In RuPh–Nd the Ru^{II}-based luminescence is substantially quenched: it is reduced in intensity by approximately 90% compared to free RuPh (Figure 2) and experiences a concomitant reduction in lifetime from 520 to 48 ns (an uncertainty of ±5% is assumed for all Ru^{II}/Os^{II}-based emission lifetimes). As the titration proceeds two luminescence components are apparent (that is, both 520 ns and 48 ns lifetime components from free RuPh and bound RuPh–Nd, see Figure 2b), with the longer component disappearing and the short component becoming dominant as the titration approaches completion. From Equation (1) this gives a Ru→Nd energy-transfer rate k_{EnT} of 1.9×10^7 s^{-1} (τ_q is the "quenched" lifetime, here 48 ns; τ_u is the "unquenched" lifetime, here 520 ns). From Equation (2) we see that the quantum yield for Ru^{II}→Nd^{III} energy transfer is 91%, in agreement with the reduction of Ru^{II}-based emission intensity.

$$k_{EnT} = \tau_q^{-1} - \tau_u^{-1} \quad (1)$$

$$\phi_{EnT} = 1 - \tau_q/\tau_u \quad (2)$$

That this reduction in Ru^{II}-based emission is genuinely due to Ru→Nd energy transfer is confirmed by two factors. Firstly, no such quenching occurs in RuPh–Gd, because Gd^{III} has no low-energy f–f states capable of acting as energy-acceptors. Secondly, sensitised Nd^{III}-based luminescence (Figure 3a) was observed at 1050 nm ($^4F_{3/2}\rightarrow{}^4I_{11/2}$) and 1330 nm ($^4F_{3/2}\rightarrow{}^4I_{13/2}$), which had a lifetime of 1.1(±0.1) μs but—more significantly—an increase of 60(±20) ns, that is, the rise-time in the Nd^{III} emission matches the decay of the Ru^{II}-based emission, confirming its origin as a sensitised emission following Ru→Nd energy transfer. Measurements of the quantum yield of the Nd^{III}-based luminescence are precluded by the presence of strong residual Ru^{II}-based

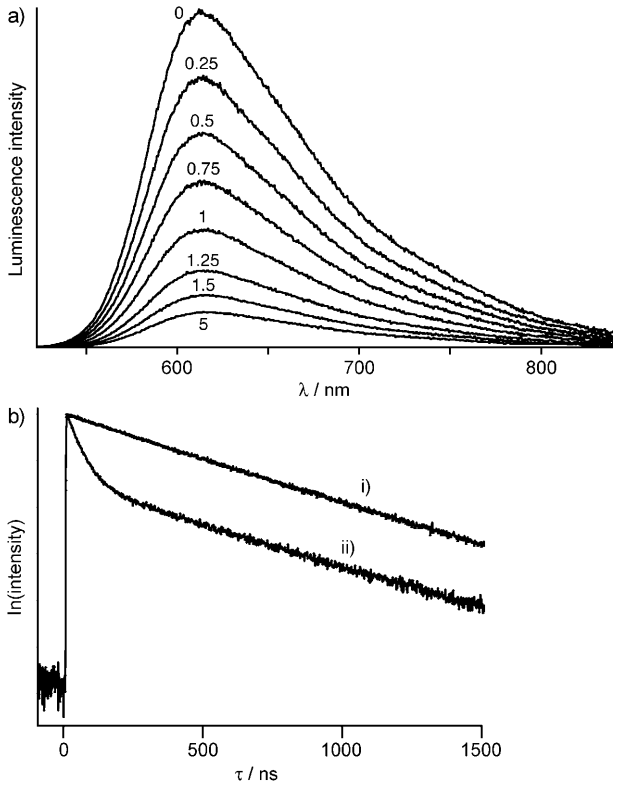

Figure 2. a) Progressive quenching of the luminescence of RuPh in CH_2Cl_2 as portions of $[Nd(tta)_3(H_2O)_2]$ are added (the number of equivalents of added $[Nd(tta)_3(H_2O)_2]$ are shown on each spectrum). b) Time-resolved measurements, showing the luminescence decay of RuPh at the start of the titration (decay i)), and the two-component decay (mixture of free RuPh; and partially-quenched RuPh–Nd; decay ii)) part of the way through the titration.

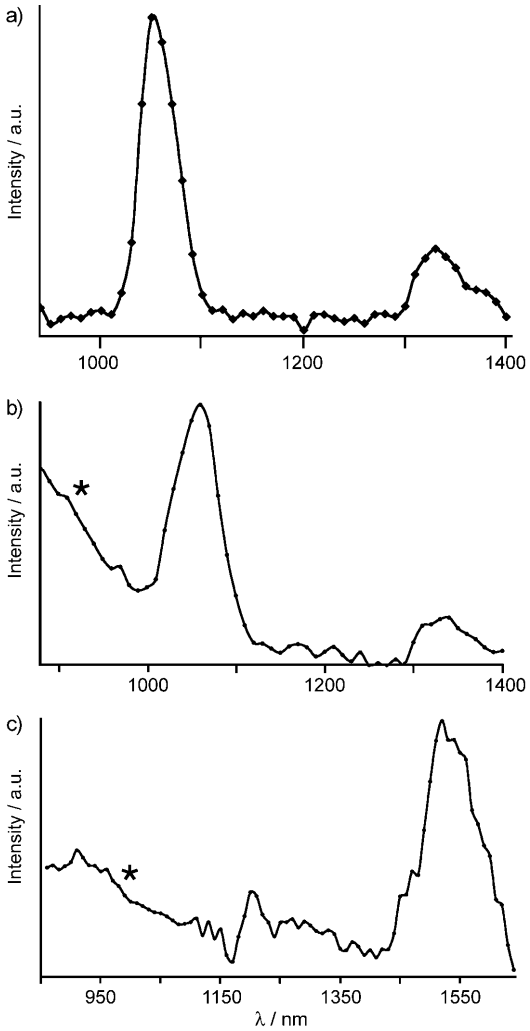

Figure 3. Sensitised Ln^{III}-based luminescence from a) Nd^{III} in RuPh–Nd, b) Nd^{III} in OsPh–Nd, and c) Er^{III} in RuPh–Er in CH_2Cl_2, following selective excitation of the Ru^{II} or Os^{II} chromophore at 460 nm. Note in b) the decaying residual Os^{II}-based luminescence, and similarly in c) the very weak decaying background of residual Ru^{II}-based luminescence; these are labelled * in each case. These spectra were recorded 250 ns after excitation to allow the Ru^{II} or Os^{II} component to decay and reveal the longer-lived Nd^{III}-based or Er^{III}-based emission features.

emission which overlaps with the high-energy end of the Nd^{III} emission spectrum, although the value can be estimated from Equation (3), in which τ_{obs} is the observed emission lifetime (1.1 μs) and τ_0 is the radiative or "natural" lifetime (0.25 ms for Nd^{III}):[22] this gives $\Phi_{Nd} \approx 4 \times 10^{-3}$, comparable to results we have obtained for other [Nd(diketonate)$_3$(diimine)] complexes.[18,23]

$$\Phi_{Ln} = \tau_{obs}/\tau_0 \quad (3)$$

In contrast, in Ru–CH_2CH_2–Nd the Ru^{II}-based luminescence is much less quenched, being reduced in lifetime from 390 to 210 ns, corresponding to a Ru→Nd energy-transfer rate of $2.2 \times 10^6\ s^{-1}$, and $\phi_{EnT} = 46\%$. The resultant sensitised Nd^{III}-based luminescence at 1050 and 1330 nm showed a rise-time of 180(±20) ns, to match the Ru^{II}-based decay (210 ns). This is apparent in Figure 3b, where a much greater intensity of residual Ru^{II}-based emission can be seen as a decaying background on which the sensitised Nd^{III}-based emission lines are superimposed. The energy-transfer rate in Ru–CH_2CH_2–Nd is therefore an order of magnitude slower than in RuPh–Nd despite occurring over a shorter distance (the maximum Ru–Nd separation in Ru–CH_2CH_2–Nd is 13.4 Å, compared to 15.6 Å in RuPh–Nd). The clear conclusion from this is that the more efficient energy transfer over a longer distance in RuPh–Nd arises from a through-bond electronic coupling mediated by the phenyl spacer, that is, a Dexter-type superexchange interaction. More detailed comments on this are as follows.

In Ru–CH_2CH_2–Nd the energy transfer is relatively slow ($2.2 \times 10^6\ s^{-1}$), which would be reasonable whichever mechanism is involved. From calculations based on the donor–acceptor spectroscopic overlap (Table 3) the critical Ru–Nd distance for Förster (dipole–dipole) energy transfer is 8.3 Å; that is, at distances much greater than this, Förster energy transfer would be too slow to compete with radiative deactivation of the Ru^{II} centre. Förster energy transfer would therefore require a highly folded conformation of the complex which brings the metal centres close together, as the Ru···Nd separation in an "opened out" conformation (13.4 Å) is 1.6 times the critical transfer distance (recall that

Table 3. Parameters used to evaluate the energy transfer features within the M–Ln dyads.[a]

Compound	k_{EnT} [s^{-1}]	d [Å]	J_F [$cm^3\,M^{-1}$]	R_c [Å]	k_F [s^{-1}]	J_D [cm]	H [cm^{-1}]	k_D [s^{-1}]
Ru–CH_2CH_2–Nd	2.2×10^6	13.4[c]	6.2×10^{-17}	8.3	1.4×10^5	1.6×10^{-4}	0.1	2.0×10^6
		9.6[b]			1.1×10^6		0.1	1.1×10^6
RuPh–Nd	1.9×10^7	15.6	6.3×10^{-17}	8.5	5.1×10^4	1.6×10^{-4}	0.3	1.9×10^7
Ru–CH_2CH_2–Er	–	13.4[c]	3.6×10^{-18}	5.2	8.4×10^3	1.5×10^{-5}	–	–
		9.6[b]			6.2×10^4		–	–
RuPh–Er	3.3×10^6	15.5	3.6×10^{-18}	5.3	3.1×10^3	1.6×10^{-5}	0.4	3.3×10^6
Os–CH_2CH_2–Nd	1.4×10^6	13.4	5.5×10^{-17}	6.4	1.9×10^5	5.2×10^{-5}	0.1	1.2×10^6
OsPh–Nd	7.1×10^6	15.5	5.3×10^{-17}	6.9	9.6×10^4	5.0×10^{-5}	0.3	7.0×10^6

[a] k_{EnT} is the experimentally observed energy-transfer rate constant; d is the predicted metal–metal separation based on molecular mechanics calculations; J_F and J_D are the Förster and Dexter overlap integrals; R_c is the Förster critical transfer distance; k_F and k_D are the calculated Förster and Dexter energy transfer rates; H is the electronic coupling value used in calculations of Dexter energy transfer ([Eq. (6)]). [b] More folded conformation (see Figure 5 b) [c] More extended conformation (see Figure 5 a).

Förster energy transfer has an d^{-6} distance dependence). Geometry optimizations performed by using molecular mechanics methods show the existence of two minimum-energy structures for the Ru–CH_2CH_2–Nd dyad, with $-CH_2-CH_2-$ bond torsion angles close to 180° (Figure 5 a) and 60° (Figure 5 b), respectively. In the more compact arrangement (Figure 5 b) the Ru–Nd separation is reduced to 9.6 Å, only a little more than the critical transfer distance, which allows Förster energy transfer to occur with a calculated efficiency $\eta_F = 0.29$. Higher-order multipolar energy transfer could also in principle contribute, because the energetically-appropriate $^4G_{5/2}$ excited state (17 700 cm^{-1}) has $|\Delta J| = 2$ with respect to the ground state.[12,13]

In such a folded conformation there would also be the possibility of a weak electronic coupling between the metal

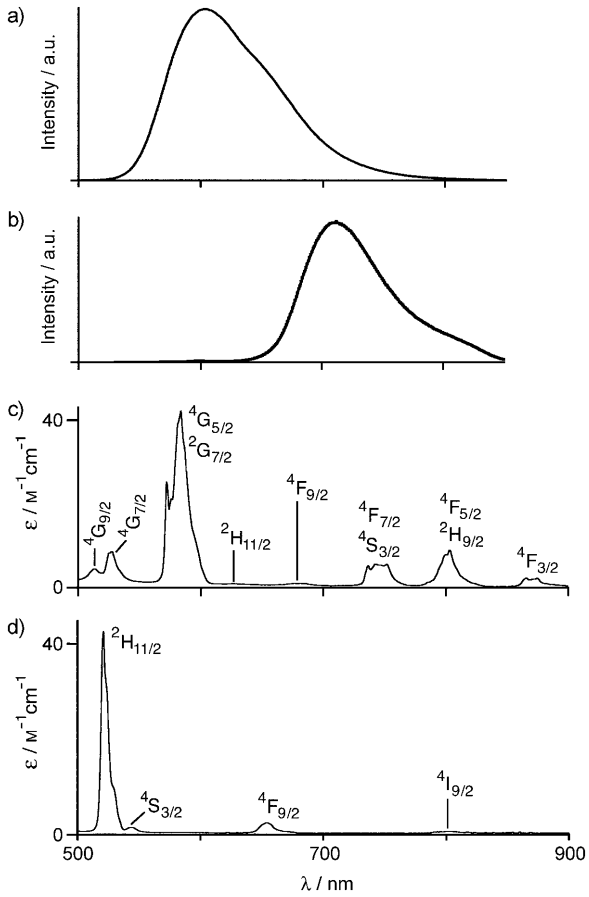

Figure 4. a) Luminescence spectrum of RuPh in CH_2Cl_2 (uncorrected). b) Luminescence spectrum of OsPh in CH_2Cl_2 (uncorrected). c) Absorption spectrum of $[Nd(tta)_3(H_2O)_2]$ in DMF between 500 and 900 nm. d) Absorption spectrum of $[Er(tta)_3(H_2O)_2]$ in DMF between 500 and 900 nm.

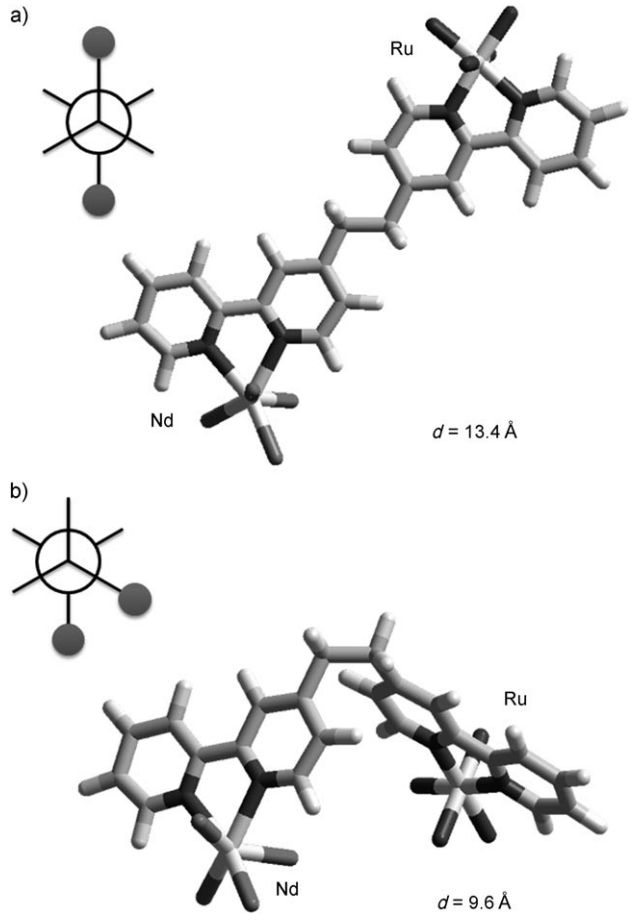

Figure 5. Minimum-energy (MM) models of the complex Ru–CH_2CH_2–Nd. a) more extended conformation; b) more folded conformation. For the sake of clarity, all atoms of the non-bridging ligands, except the coordinating ones (O and N) surrounding the metal centers, have been removed from the picture. The relevant intermetal distances are reported for the different conformations.

centres due to interaction of the peripheries of their aromatic ligands (bipyridyl and tta), allowing some Dexter energy transfer with an efficiency $\eta_D = 0.46$. The corresponding electronic interaction factor, $H = 0.1\ cm^{-1}$, is typical of very weakly interacting components. Several excited states of the Nd^{III} in the 11000–20000 cm^{-1} range match the required $|\Delta J| = 0, 1$ selection rule for Dexter energy transfer, as mentioned in more detail below.

It is therefore not possible to say definitively which energy-transfer mechanism is operative in Ru–CH_2CH_2–Nd, but it is clearly slow compared to RuPh–Nd and only likely to happen in highly folded conformers which bring the metal centres into proximity.

In RuPh–Nd the presence of the conjugated phenylene bridge increases the energy-transfer rate by an order of magnitude despite the rigidity of the bridge which imposes a larger Ru–Nd separation of 15.6 Å (with no possibility for the folding that could occur in Ru–CH_2CH_2–Nd). Since the Ru–Nd separation is now essentially fixed at more than double the Förster critical distance, energy transfer can *only* occur by the higher-order multipolar or exchange mechanisms. We can easily rule out the former on empirical grounds: since any multipolar contribution to energy transfer was only modestly efficient in Ru–CH_2CH_2–Nd (energy-transfer rate, $2.2\times10^6\ s^{-1}$; ϕ_{EnT}, 46%), and has a d^{-8} (or worse, depending on the multipoles involved) distance dependence, multipolar energy transfer can only make a negligible contribution to the faster energy transfer over a greater distance in RuPh–Nd. Therefore we can confidently ascribe Ru→Nd energy transfer over 15.6 Å in RuPh–Nd to a Dexter-type exchange process mediated by the orbitals of the conjugated phenyl spacer, that is, a superexchange process.

The selection rule for exchange energy transfer, that $|\Delta J| = 0, 1$ with respect to the $^4I_{9/2}$ ground state of Nd^{III},[12,13] suggests that direct involvement of some f–f excited states of Nd^{III} in the energy-transfer process can be ruled out. Like any selection rule however it only applies to the extent that the wavefunctions are pure, that is, that the *L*, *S* and *J* descriptors on which the selection rules are based are accurate. Any mixing of the f–f levels with other states such as 5d–4f states, or MLCT states, will provide a mechanism for selection rules to be relaxed. But if we assume this selection rule applies completely we find that the emissive $^4F_{3/2}$ level, for example, has $|\Delta J| = 3$ with respect to the ground state and therefore cannot be populated directly by any energy-transfer mechanism. However there are several f–f states available which can be directly populated by Dexter energy transfer: in ascending order, $^2H_{9/2}$, $^4F_{7/2}$, $^4F_{9/2}$, $^2H_{11/2}$ and $^2G_{7/2}$ for example all have $|\Delta J| = 0$ or 1 with respect to the ground state, and lie between 12800 and 17600 cm^{-1} (energy level values taken from free-ion spectra of the Nd^{III} ion[24]) such that they have some overlap with the ^{3}MLCT luminescence spectrum of the Ru^{II} energy-donor (Figure 4). For both RuPh and Ru–CH_2CH_2 the ^{3}MLCT energy (taken from the emission maximum at 77 K) is 17200 cm^{-1}.

iii) Comparison of RuPh–Nd with $RuPh_2$–Nd: In the more extended unsaturated complex $RuPh_2$–Nd (Ru···Nd separation, 19.9 Å) the Ru^{II}-based luminescence is partially quenched, from 460 ns in $RuPh_2$ to 256 ns in $RuPh_2$–Nd. Thus Ru→Nd energy transfer is still occurring over this distance, but with a reduced rate constant ($1.7\times10^6\ s^{-1}$) and quantum yield (44%) because of the greater distance involved and the consequent attenuation of electronic coupling. The resultant sensitised Nd^{III}-based emission showed a growth of approximately 200-(±30) ns, in reasonable agreement with the partially-quenched Ru^{II}-based decay (256 ns). By analogy with the discussion above for RuPh–Nd, this can only be occurring by a bridging-ligand mediated exchange mechanism.

This decreased rate of Ru→Nd energy transfer compared to RuPh–Nd may be accounted for by Equation (4), which shows how the rate of exchange-based energy transfer through a bridging ligand decays exponentially with distance (*d*) to an extent dependent on an attenuation coefficient β (units of $Å^{-1}$) which is a measure of how the metal–metal electronic coupling diminishes with distance. *A* is a constant.

$$k_{EnT} = A\,e^{-\beta d} \qquad (4)$$

We can, to a reasonable approximation, take the Dexter donor–acceptor spectroscopic overlap to be the same between RuPh–Nd and $RuPh_2$–Nd. Given a decrease in energy transfer rate from $1.9\times10^7\ s^{-1}$ to $1.7\times10^6\ s^{-1}$ as the Ru···Nd separation increases from 15.6 to 19.9 Å, from Equation (4) we arrive at a value of the attenuation coefficient β of 0.56 $Å^{-1}$ associated with the additional phenylene spacer in $RuPh_2$–Nd. This is entirely consistent with what others have determined for the electronic attenuation coefficient of phenylene-spaced conjugated bridging ligands in dinuclear transition metal complexes,[20,25] and provides additional support for the exchange mechanism for energy transfer operating here.

Exchange energy transfer over this sort of distance is unusual in lanthanide(III) complexes precisely because of the exponential distance dependence. The lanthanide donor–organic dye acceptor pairs commonly used for long-range FRET studies in biological systems, for example,[15] are optimised for resonance energy transfer because donors such as Tb^{III} have high luminescence quantum yields and long lifetimes, and the acceptors have broad absorption bands with high extinction coefficients.[15e,f] This results in Förster spectroscopic overlap integrals that are many orders of magnitude higher than those calculated for our systems (Table 3), and critical transfer distances approaching 100 Å in some cases.[15e,f] In RuPh–Nd and $RuPh_2$–Nd however the energy donor has a low quantum yield (3–4%) and the f–f lanthanide absorptions are narrow with tiny extinction coefficients, a situation which is inimical to Förster energy transfer, hence the critical transfer distances of 8.5 Å or less. A dipole–quadrupole contribution to resonance energy transfer may be more allowed (depending which excited f–f states are involved) but has a more rapid decay with distance.

Dexter-type exchange energy transfer is therefore the only option that remains in RuPh–Nd and $RuPh_2$–Nd and is made possible by the presence of the long conjugated bridge which permits electronic coupling, a structural feature which is notably absent in FRET-type systems.[15]

iv) Other Ru^{II}–Ln^{III} combinations: effect of the lanthanide: Other Ru^{II}–Ln^{III} combinations show generally comparable behaviour (Table 2). It is clear that Er^{III} and Yb^{III} are both less effective energy-acceptors than Nd^{III} because neither of them give any detectable quenching of the Ru^{II}-based luminescence in Ru–CH_2CH_2–Ln. Note that between Ru–CH_2CH_2–Nd and Ru–CH_2CH_2–Er the Förster spectroscopic overlap integral decreases by an order of magnitude, with a reduction in the critical transfer distance to just 5.2 Å, because Er^{III} has fewer f–f absorptions that overlap with the Ru^{II}-based luminescence (Figure 4). The Dexter overlap integral has likewise decreased by an order of magnitude compared with Ru–CH_2CH_2–Nd. The absence of quenching of the Ru^{II} centre in Ru–CH_2CH_2–Er by any mechanism is therefore entirely understandable.

In the RuPh–Ln dyads the effectiveness of the different Ln^{III} species as energy-acceptors is Nd > Er > Yb, with residual Ru^{II}-based lifetimes of 48, 190 and 250 ns respectively. This gives steadily-decreasing Ru→Ln energy-transfer rates of $1.9\times10^7\ s^{-1}$ (to Nd; $\phi_{EnT}=91\,\%$), $3.3\times10^6\ s^{-1}$ (to Er; $\phi_{EnT}=63\,\%$) and $2.1\times10^6\ s^{-1}$ (to Yb; $\phi_{EnT}=52\,\%$), as the donor–acceptor overlap decreases due to the reduced availability of f–f states on the Ln^{III} ions. This exactly mirrors what we have seen in $[Ru(bipy)(CN)_4]^{2-}$–Ln^{III} coordination networks.[26] Again we can be sure that exchange energy transfer is operating in these cases because i) the critical distances for Förster energy transfer (for example, 5.3 Å for Ru^{II}/Er^{III}) are much less than the distance across this rigid bridging ligand, and ii) addition of the conjugated spacer increases energy-transfer rates substantially despite increasing the separation between donor and acceptor. The expected sensitised Ln^{III}-based luminescence is seen in each case: for Yb^{III}, at 980 nm (superimposed on the tail of the strong residual Ru^{II}-based emission, such that reliable lifetime/quantum yield measurements are not possible) and for Er^{III}, at 1530 nm (characteristically very weak, see Figure 3c).

The Dexter energy-transfer mechanism requires the energy-accepting levels on the Ln^{III} ions to have $|\Delta J|=0,1$ with respect to the ground state; again, we emphasise that this applies only to the extent that the f–f states are "pure". For Yb^{III} the selection rule is inevitably obeyed because the ground state is $^2F_{7/2}$ and the only excited state is $^2F_{5/2}$, that is, $|\Delta J|=1$. For Er^{III} the situation is however less obvious because application of this selection rule apparently prohibits any of the f–f states in the relevant region from participating: none of the levels between 10000 and 20000 cm^{-1} (in ascending order: $^4I_{11/2}$, $^4I_{9/2}$, $^4F_{9/2}$, $^4S_{3/2}$, $^2H_{11/2}$) have $|\Delta J|=0,1$ with respect to the ground state ($^4I_{15/2}$). In fact the $|\Delta J|$ values with respect to the ground state are 2, 3, 3, 6, and 2 respectively, implying that the $^4I_{11/2}$, $^4S_{3/2}$ and $^2H_{11/2}$ states are allowed to participate in multipolar energy transfer but this has been ruled out as it does not happen over a shorter distance in Ru–CH_2CH_2–Er.

The only f–f state of Er^{III} that fulfils the formal selection rule for Dexter energy transfer is the luminescent level $^4I_{13/2}$ at approximately 6500 cm^{-1} ($|\Delta J|=1$) which is however so low in energy that any spectroscopic overlap with the low-energy tail of Ru^{II}-based or Os^{II}-based emission must be negligible, certainly less than that which occurs in Ru^{II}–Yb^{III} and Os^{II}–Yb^{III} dyads (the sole Yb^{III}-based excited state is at 10200 cm^{-1}). Yet, Er^{III} is clearly a better energy-acceptor than Yb^{III} based on the energy-transfer rates calculated above. So we have the situation that Ru→Er energy transfer is clearly occurring in RuPh–Er (with $k_{EnT}=3.3\times10^6\ s^{-1}$), yet it is apparently forbidden by any of the Coulombic mechanisms on the grounds of distance (critical transfer distance 5.3 Å, compared to an actual Ru···Er distance of 15.6 Å) and by comparison with Ru–CH_2CH_2–Er; and it is also forbidden by the Dexter mechanism on the grounds of the selection rules based on permitted $|\Delta J|$ values.

The only reasonable explanation for this is the one alluded to above: the formal selection rules only apply to the extent that *J* is a good quantum number for the 4f levels involved, and the wavefunctions are pure without mixing from allowed charge-transfer or 4f–5d transitions. The Russell–Saunders coupling scheme is known to break down for heavier lanthanide(III) ions such as Er^{III}. Indeed the presence of any spectroscopic overlap at all relies on "forbidden" f–f absorptions having non-zero intensity because of the various ways in which the selection rules applying to f–f transitions can be circumvented. The magnitude of the donor–acceptor spectroscopic overlap (Table 3) is therefore a good indication of the extent to which the selection rules can be avoided because the f–f states are not pure.

v) Os^{II}–Ln^{III} complexes: The behaviour of the Os^{II}/Ln^{III} systems is also instructive. The intensity of Os^{II}-based luminescence from OsS–Nd is reduced by about 3% compared to free Os–CH_2CH_2, a degree of quenching that is at the limit of significance. Likewise the luminescence lifetime is barely reduced, from 62 to 57 ns. Application of Equation (5) to these values gives an Os→Nd energy-transfer rate of $1.4\times10^6\ s^{-1}$; however an uncertainty of 5% in each separate measurement gives a range of possible values for the energy-transfer rate from zero to $3\times10^6\ s^{-1}$. We can say that the extent of Os→Nd energy transfer is almost negligible ($\phi_{EnT}=3\,\%$ based on quenching of Os^{II}-based luminescence intensity) and the rate is at best $\approx10^6\ s^{-1}$, that is, comparable to, or slower than, the Ru→Nd energy-transfer rate in Ru–CH_2CH_2–Nd ($2.2\times10^6\ s^{-1}$).

Although the Os→Nd energy transfer in Os–CH_2CH_2–Nd is minimal, careful examination of time-resolved emission spectra for Os–CH_2CH_2–Nd in the near-IR region shows a weak shoulder at approximately 1060 nm superimposed on the tail of the much stronger Os^{II}-based emission (Figure 3b). This feature persists for considerably longer than the Os^{II}-based emission, and is still just visible after 1 μs, at which time the Os^{II}-based emission has completely decayed.

Although rise/decay times cannot be determined we can assign this feature at 1050 nm to weak sensitised Nd^{III}-based emission, proof of the occurrence of Os→Nd energy transfer. We note that even if the Ru→Nd and Os→Nd energy-transfer rates may be comparable in Ru–CH_2CH_2–Nd and Os–CH_2CH_2–Nd (the maximum possible Os→Nd energy-transfer rate based on the uncertainty values quoted above is $3\times10^6\,s^{-1}$, comparable to the Ru→Nd energy-transfer rate of $2.2\times10^6\,s^{-1}$), the *extent* of Os→Nd energy transfer, based on the degree of quenching of the Os^{II} luminescence, is minimal because of the shorter lifetime of the Os^{II}-based donor. Thus, Os→Nd energy transfer is a relatively insignificant deactivation pathway for Os^{II} in Os–CH_2CH_2–Nd because it is not competitive with the other Os^{II}-centred radiative and non-radiative deactivation pathways. Table 3 shows that the Förster spectroscopic overlap integral for Os–CH_2CH_2–Nd is comparable (lower by 11%) to that for Ru–CH_2CH_2–Nd, but the critical transfer distance for Förster energy transfer, which includes contributions from the lifetime and quantum yield of the donor, is reduced from 8.3 to 6.4 Å. Also, the Dexter overlap integral is reduced by a factor of three compared to Ru–CH_2CH_2–Nd, so Dexter energy transfer is also less likely.

OsPh–Nd however shows significant quenching of the Os^{II}-based luminescence (lifetime reduced from 80 to 51 ns), giving an Os→Nd energy-transfer rate of $7.1\times10^6\,s^{-1}$ ($\phi_{EnT}=36\%$), about one third of the Ru→Nd energy-transfer rate in RuPh–Nd. Sensitised Nd^{III}-based emission at 1050 and 1330 nm is clearly visible ($\tau=1.1(\pm0.2)$ μs), but superimposed on the long-wavelength tail of residual Os^{II}-based emission such that its rise time cannot be measured (the rise-time component of the Nd^{III}-based emission at 1050 nm, expected to be 51 ns, will be superimposed on the 51 ns decay of the Os^{II}-based residual emission). Again (as for the comparison between Ru–CH_2CH_2–Nd and RuPh–Nd) the Os→Nd energy transfer must occur by a ligand-mediated exchange mechanism, because of the near-absence of energy transfer over a shorter distance in Os–CH_2CH_2–Nd when a saturated spacer was involved. In this case it is clear that Os→Nd energy transfer ($7.1\times10^6\,s^{-1}$) is slower than Ru→Nd energy transfer ($1.9\times10^7\,s^{-1}$), which must be solely due to the reduced Dexter spectroscopic overlap integrals (5×10^{-5} cm for OsPh–Nd, compared to 1.6×10^{-4} cm for RuPh–Nd). Actually the Dexter overlap integral is a factor of three lower for OsPh–Nd than RuPh–Nd, in good agreement with the relative rates of energy transfer, which further supports the exchange-based mechanism for energy transfer in these complexes.

vi) Comparison of Ru^{II} versus Os^{II} complexes as energy donors: It is clear that, in these dyads, $[Os(bipy)_3]^{2+}$ is a poorer energy-donor than $[Ru(bipy)_3]^{2+}$ for sensitisation of near-IR luminescence from Nd^{III}. According to the calculations in Table 3, in every case the overlap integrals for both Förster and Dexter energy transfer are smaller for the Os–Ln pair than for the Ru–Ln pair with the same Ln^{III} ions (for Ln = Nd, Er). Even when this difference is not large and the rates of Ru→Ln versus Os→Ln energy transfer may be similar, the quantum yield for Os→Ln energy transfer will be less because of the more rapid radiative deactivation of the Os^{II} unit.

This observation is, interestingly, in exact contrast to what we have recently observed when comparing $[Ru(bipy)(CN)_4]^{2-}$–Ln^{III} and $[Os(bipy)(CN)_4]^{2-}$–Ln^{III} coordination networks based on short M–CN–Ln bridges, in which Os→Ln energy transfer was *faster* than Ru→Ln energy transfer across the same distance.[27] Thus, it is not possible to generalise that either Ru^{II} or Os^{II} donors are better sensitisers of a particular Ln^{III} ion; this will depend on the balance between the many different factors that contribute to the different energy-transfer mechanisms in different systems (spectroscopic properties, electronic couplings, intercomponent distance etc.).

Conclusion

We have shown that Coulombic energy transfer from $[M(bipy)_3]^{2+}$ (M = Ru, Os) to the near-IR emissive Ln^{III} ions can essentially be ignored in these complexes. Förster (dipole–dipole) energy transfer can be ruled out because of the small critical transfer distances involved, with the possible exception of Ru–CH_2CH_2–Nd for which the critical transfer distance is approximately 8.5 Å, close to what is attainable in a highly folded conformation of the flexible bridging ligand. Higher-order multipolar contributions to energy transfer are in principle possible but, at most, make a small contribution to energy transfer in Ru–CH_2CH_2–Nd across the short saturated bridge and are clearly insignificant in other Ru–CH_2CH_2–Ln and Os–CH_2CH_2–Ln complexes. The high distance dependence of this mechanism means therefore that it cannot contribute to the much faster energy transfer which occurs over greater distances in RuPh–Ln and $RuPh_2$–Nd.

The presence of Ru→Ln energy transfer in RuPh–Ln (Ln = Nd, Er, Yb) and in $RuPh_2$–Nd and OsPh–Nd can be ascribed unequivocally to a Dexter-type superexchange process mediated by the conjugated bridging ligands, with the rate depending on i) the availability of f–f states on the lanthanide of the appropriate energy, and ii) whether Ru^{II} or Os^{II} is the donor. The distance dependence of the energy transfer (comparison of RuPh–Nd and $RuPh_2$–Nd), and the correlation of energy-transfer rates with Dexter overlap integrals (comparison of RuPh–Nd and OsPh–Nd) both provide support for this mechanism being operative. The rates of energy transfer that we observed are much higher than in other d–f systems based on dinuclear triple helicates where there is no conjugated bridging ligand: for example, Ru^{II}→Nd^{III} energy transfer was reported to occur over approximately 9 Å with a rate of $2.3\times10^6\,s^{-1}$,[28] compared to our ligand-mediated Ru^{II}→Nd^{III} exchange energy-transfer rate of $1.9\times10^7\,s^{-1}$ over a distance of 15.6 Å.

We also found that $[Os(bipy)_3]^{2+}$ is a poorer energy-donor than $[Ru(bipy)_3]^{2+}$ in these dyads, with only OsPh–Nd show-

ing evidence for significant Os→Ln energy transfer. Finally, we note that, in these cases, the donor–acceptor spectroscopic overlap integrals, which implicitly take account of the fact that f–f states are not pure, are a better guide to the presence/absence of energy transfer than the formal selection rules, which do not.

Experimental Section

General details: ^{1}H NMR spectra were recorded on a Bruker AC-250 spectrometer. Electrospray mass spectra were recorded on a Waters LCT instrument. UV/Vis absorption spectra were measured on a Cary 50 spectrophotometer. Metal salts, organic ligands and other reagents were purchased from Aldrich and used as received.

Photophysical measurements and calculations: Luminescence spectra were measured on a Jobin-Yvon Fluoromax 4 fluorimeter by using air-equilibrated CH_2Cl_2 solutions at room temperature, or EtOH/MeOH (4:1, v/v) glasses at 77 K. Ru^{II}-based and Os^{II}-based luminescence lifetimes were measured with an Edinburgh Instruments "Mini-τ" luminescence lifetime spectrometer, equipped with a 405 nm pulsed diode laser as excitation source and a cooled Hamamatsu-R928 PMT detector (wavelength selection at the detector was by means of 50 nm bandpass filters; for Ru^{II} complexes a 575–625 nm bandpass filter was used, and for Os^{II} complexes a 625–675 nm bandpass filter was used). Quantum yields for Ru^{II}- and Os^{II}-based luminescence were determined by using the method of Demas and Crosby,[29] and by using $[Ru(bpy)_3]^{2+}$ as a standard ($\Phi = 2.8\times10^{-2}$ in aerated water).[30]

Instrumentation used for steady-state and time-resolved luminescence measurements on the lanthanide-based emission in the near-IR region, and methods used for data analysis, have been described previously.[23]

For the calculation of the energy transfer rates based on Förster and Dexter mechanisms (Table 3), corrected donor emission spectra and acceptor absorption spectra in molar absorptivity units (after conversion from wavelengths to wavenumbers) were used. The intermetallic M–Ln distance (M = Ru and Ln = Nd, Er) was taken as the interchromophoric distance and was calculated from optimized molecular structures in vacuum. Computations of the energy transfer rate constants for Förster and Dexter mechanisms ([Eq. (5) and (6)]) and the relevant spectroscopic overlap integrals ([Eq. (7) and (8)]) were performed with home-developed routines for MATLAB 5.2 (The MatWorks, Inc.). The symbols used in Equations (5)–(8) are as follows: τ = luminescence lifetime; ϕ = luminescence quantum yield; κ^2 the orientation factor; d_{MM} is the metal–metal separation; h is the Planck's constant; other symbols are defined in the caption to Table 3. For the Förster energy-transfer rates, the orientation factor κ^2 was taken as 2/3 for statistical reasons.[31] Geometries of the complexes were obtained by using the molecular mechanics method with the MM+ force field in HYPERCHEM 8.0 (Hypercube, Inc.).

$$k_{en}^{F} = \frac{8.8\times10^{-25}K^2\phi}{n^4\tau {d_{MM}}^6}J_F \quad (5)$$

$$k_{en}^{D} = \frac{4\pi^2H^2}{h}J_D \quad (6)$$

$$J_F = \frac{\int F(\bar{\nu})\varepsilon(\bar{\nu})/\bar{\nu}^4 d\bar{\nu}}{\int F(\bar{\nu})d\bar{\nu}} \quad (7)$$

$$J_D = \frac{\int F(\bar{\nu})\varepsilon(\bar{\nu})d\bar{\nu}}{\int F(\bar{\nu})d\bar{\nu}\int \varepsilon(\bar{\nu})d\bar{\nu}} \quad (8)$$

Syntheses: The following compounds were prepared according to literature methods: 4-(4-bromophenyl)-2,2′-bipyridine (bpy-Ph-Br),[32] 4-(4-phenyl-boronic acid)-2,2′-bipyridine [bpy-Ph-B(OH)$_2$],[33] 1,4-bis[4-(2,2′-bipyridyl)]benzene (bpy-Ph-bpy),[34] Ru–CH_2CH_2,[35] Os–CH_2CH_2,[36] [Ru(tBu$_2$bpy)$_2$Cl$_2$],[37] [Ru(bpy)$_2$Cl$_2$],[38] [Os(bpy)$_2$Cl$_2$],[39] and the [Ln(tta)$_3$(H$_2$O)$_2$] complexes.[40]

[Ru(tBu$_2$bpy)$_2$(bpy-Ph-Br)](PF$_6$)$_2$: This compound was prepared by using a modified literature procedure.[32] A mixture of [Ru(tBu$_2$bpy)$_2$Cl$_2$] (0.182 g, 0.26 mmol) and bpy-Ph-Br (0.080 g, 0.26 mmol) in EtOH (20 mL) was degassed by purging with N_2 for 5 min before being refluxed under an N_2 atmosphere for 2 h. The solvent was then removed on a rotary evaporator and the crude product was purified by column chromatography on silica gel (MeCN/H$_2$O/sat. aq. KNO$_3$ 15:2:1). The fractions containing the main red band were combined and the solvent was removed. The residue was then re-dissolved in a mixture of water (2 mL) and MeOH (0.5 mL), and a saturated aqueous solution of NH_4PF_6 (1 mL) was added affording the desired product as red-orange precipitate which was collected by filtration, washed with water (3×2 mL) and dried. Yield: 0.223 g (69 %). ^{1}H NMR (250 MHz, [D$_6$]acetone): δ = 9.18 (d, 1H); 9.07 (d, 1H); 8.23 (m, 1H); 8.10–7.75 (overlapping multiplets, 11H); 7.65–7.52 (m, 5H); 1.42 (s, 18H) 1.40 ppm (s, 18H); MS (ES$^+$): m/z 1093 $[M-PF_6]^+$, 474 $[M-2PF_6]^{2+}$, 466 $[M-CH_3-2PF_6]^{2+}$, 459 $[M-2CH_3-2PF_6]^{2+}$, 451 $[M-3CH_3-2PF_6]^{2+}$; elemental analysis calcd (%) for $C_{52}H_{59}BrF_{12}N_6P_2Ru$: C 50.4, H 4.8, N 6.8; found C 50.4, H 5.2, N 6.9.

RuPh$_2$: This compound was prepared by using a modification of a literature procedure.[33] A dry Schlenk tube was charged with [Ru(tBu$_2$bpy)$_2$(bpy-Ph-Br)](PF$_6$)$_2$ (0.213 g, 0.17 mmol), bpy-Ph-B(OR)$_2$ (0.200 g, 0.55 mmol) and DMF (20 mL). The solution was degassed by the freeze-pump-thaw technique, and [Pd(PPh$_3$)$_4$] (4 mol %) was added. The Schlenk tube was sealed and the reaction mixture heated at 120 °C for 24 h. After the end of the reaction the solvent was evaporated to afford a red solid, which was purified by column chromatography on silica gel (MeCN/H$_2$O/sat. aq. KNO$_3$ 35:2:1) as eluent. The fractions containing the second orange band were combined and the solvent was removed in a rotary evaporator. The residue was re-dissolved in a mixture of water (2 mL) and methanol (0.5 mL), and a saturated aqueous solution of NH_4PF_6 (1 mL) was added to afford the desired product as a red-orange precipitate which was collected by filtration, washed with water (3×2 mL) and dried. Yield: 0.19 g (80 %). ^{1}H NMR (250 MHz, [D$_3$]MeCN): δ = 8.89–8.75 (m, 5H), 8.55–8.45 (m, 5H), 8.10–7.90 (m, 9H), 7.80–7.60 (m, 9H), 7.5–7.39 (m, 6H), 1.43 (s, 18H), 1.41 ppm (s, 18H); MS (ES$^+$): m/z: 1245.2 $[M-PF_6]^+$, 550.1 $[M-2PF_6]^{2+}$; elemental analysis calcd (%) for $C_{68}H_{70}F_{12}N_8P_2Ru$: C 58.7, H 5.1, N 8.1; found C 58.5, H 5.3, N 7.9.

RuPh: A mixture of [Ru(bpy)$_2$Cl$_2$] (0.110 g, 0.21 mmol) and bpy-Ph-bpy (0.440 g, 1.14 mmol) in EtOH (20 mL) was degassed by purging with N_2 for 5 min before being heated to reflux under N_2 for 2 h. The solvent was then removed in a rotary evaporator, water (1 mL) was added to the residue, and any insoluble unreacted ligand was removed by filtration. The orange-red filtrate was evaporated to dryness, and the residue was purified by column chromatography on silica gel (MeCN/H$_2$O/sat. aq. KNO$_3$ 25:2:1) as eluent. The desired mononuclear complex eluted in the first orange-red band, which was collected and the solvent was removed in a rotary evaporator. The residue was re-dissolved in a mixture of water (2 mL) and methanol (0.5 mL), and a saturated aqueous solution of NH_4PF_6 (1 mL) was added, affording the desired product as red-orange precipitate which was collected by filtration, washed with water (3× 2 mL) and dried. Yield: 0.06 g (26 %). ^{1}H NMR (250 MHz, [D$_6$]acetone): δ = 9.23 (d, 1H); 9.11 (d, 1H); 8.90–8.67 (m, 7H); 8.54 (d, 1H); 8.30–8.04 (m, 15H); 7.96 (m, 2H); 7.81 (dd, 1H); 7.60 (m, 5H); 7.46 ppm (m, 1H); MS (ES$^+$): m/z: 945.0 $[M-PF_6]^+$, 400.0 $[M-2PF_6]^{2+}$; elemental analysis calcd (%) for $C_{46}H_{34}F_{12}N_8RuP_2$: C 50.7, H 3.1, N 10.3; found: C 50.4, H 3.1, N 10.4.

OsPh: This was prepared and purified in the same way as RuPh, except by using [Os(bpy)$_2$Cl$_2$] as the starting material, 1:1 EtOH/toluene as the solvent, and heating the reaction mixture at reflux for 48 h under N_2. It was isolated as a dark green solid. Yield: (30 %). ^{1}H NMR (250 MHz, [D$_3$]MeCN): δ = 8.80–8.68 (m, 5H); 8.55–8.45 (m, 5H); 8.08 (s, 4H); 8.00–7.82 (m, 6H); 7.80–7.60 (m, 8H) 7.48 (m, 1H) 7.40–7.30 ppm (m, 5H); MS (ES$^+$): m/z: 1035.1 $[M-PF_6]^+$, 445.1 $[M-2PF_6]^{2+}$; elemental analysis calcd (%) for $C_{46}H_{34}F_{12}N_8OsP_2$: C 46.9, H 2.9, N 9.5; found C 46.4, H 3.1, N 9.3.

Acknowledgements

We thank the EPSRC (UK), EU-COST action D31, and the CNR Project PM.P04.010 (ITA) for financial support. We also thank our colleague Francesco Barigelletti for helpful discussions during the preparation of the manuscript, and the referees of the first version of the manuscript for some helpful suggestions.

[1] M. D. Ward, *Coord. Chem. Rev.* **2007**, *251*, 1663.
[2] D. L. Dexter, *J. Chem. Phys.* **1953**, *21*, 836.
[3] N. Sabbatini, M. Guardigli, J.-M. Lehn, *Coord. Chem. Rev.* **1993**, *123*, 201.
[4] S. Faulkner, J. L. Matthews in *Comprehensive Coordination Chemistry Vol. 9*, 2nd ed., (Ed.: M. D. Ward), Elsevier, **2004**, pp. 913–944.
[5] a) G. A. Hebbink, S. I. Klink, L. Grave, P. G. B. O. Alink, F. C. J. M. v an Veggel, *ChemPhysChem* **2002**, *3*, 1014; b) A. I. Voloshin, N. M. Shavaleev, V. P. Kazakov, *J. Photochem. Photobiol. A* **2000**, *131*, 61.
[6] a) T. Lazarides, M. A. H. Alamiry, H. Adams, S. J. A. Pope, S. Faulkner, J. A. Weinstein, M. D. Ward, *Dalton Trans.* **2007**, 1484; b) S. Faulkner, B. P. Burton-Pye, T. Khan, L. R. Martin, S. D. Wray, P. J. Skabara, *Chem. Commun.* **2002**, 1668; c) A. Beeby, S. Faulkner, J. A. G. Williams, *J. Chem. Soc. Dalton Trans.* **2002**, 1918; d) W. D. Horrocks, Jr., J. P. Bolender, W. D. Smith, R. M. Supkowski, *J. Am. Chem. Soc.* **1997**, *119*, 5972.
[7] For a review on long-range energy-transfer mechanisms, see: G. D. Scholes, *Annu. Rev. Phys. Chem.* **2003**, *54*, 57.
[8] For representative recent examples, see: a) K. Pettersson, A. Kyrychenko, E. Rönnow, T. Ljungdahl, J. Mårtensson, B. Albinsson, *J. Phys. Chem. A* **2006**, *110*, 310; b) S. Wallin, L. Hammarström, E. Blart, F. Odobel, *Photochem. Photobiol. Sci.* **2006**, *5*, 828; c) A. Elghayoury, A. Harriman, R. Ziessel, *J. Phys. Chem. A* **2000**, *104*, 7906; d) V. Russo, C. Curutchet, B. Mennucci, *J. Phys. Chem. B* **2007**, *111*, 853; e) E. K. L. Yeow, D. J. Haines, K. P. Ghiggino, M. N. Paddon-Row, *J. Phys. Chem. A* **1999**, *103*, 6517; f) S. Welter, F. Lafolet, E. Cecchetto, F. Vergeer, L. De Cola, *ChemPhysChem* **2005**, *6*, 2417; g) S. Welter, N. Salluce, P. Belser, M. Groenefeld, L. De Cola, *Coord. Chem. Rev.* **2005**, *249*, 1360; h) A. Harriman, A. Khatyr, R. Ziessel, A. Benniston, *Angew. Chem.* **2000**, *112*, 4457; *Angew. Chem. Int. Ed.* **2000**, *39*, 4287.
[9] G. L. Closs, J. R. Miller, *Science* **1988**, *240*, 440.
[10] Th. Förster, *Discuss. Faraday Soc.* **1959**, *27*, 7.
[11] a) C. K. Jörgensen, B. R. Judd, *Mol. Phys.* **1964**, *8*, 281; b) R. D. Peacock, *Struct. Bonding (Berlin)* **1975**, *22*, 83.
[12] O. L. Malta, *J. Lumin.* **1997**, *71*, 229.
[13] a) G. F. De Sa, O. L. Malta, C. de Mello Donega, A. M. Simas, R. L. Longo, P. A. Santa-Cruz, E. F. da Silva Jr. , *Coord. Chem. Rev.* **2000**, *196*, 165; b) G. A. Hebbink, L. Grave, L. A. Woldering, D. N. Reinhoudt, F. C. J. M. van Veggel, *J. Phys. Chem. A* **2003**, *107*, 2483; c) F. R. G. e Silva, O. L. Malta, C. Reinhard, H.-U. Güdel, C. Piguet, J. E. Moser, J.-C. G. Bünzli, *J. Phys. Chem. A* **2002**, *106*, 1670.
[14] A. van der Avoird, P. E. S. Wormer, F. Mulder, R. M. Berns, *Top. Curr. Chem.* **1980**, *93*, 1.
[15] a) L. C. Courrol, F. R. de Oliveira Silva, L. Gomes, N. D. Vieria Júnior, *J. Lumin.* **2007**, *122–123*, 288; b) P. R. Selvin, J. E. Hearst, *Proc. Natl. Acad. Sci. USA* **1994**, *91*, 10024; c) M. A. Baldo, M. E. Thompson, M. R. Forrest, *Pure Appl. Chem.* **1999**, *71*, 2095; d) K. W. Vogel, K. L. Vedvik, *J. Biomol. Screening* **2006**, *11*, 439; e) C. A. Royer, *Chem. Rev.* **2006**, *106*, 1769; f) P. R. Selvin, *Annu. Rev. Biophys. Biomol. Struct.* **2002**, *31*, 275.
[16] S. Campagna, F. Puntoriero, F. Nastasi, G. Bergamini, V. Balzani, *Top. Curr. Chem.* **2007**, *280*, 117.
[17] D. Kumaresan, K. Shankar, S. Vaidya, R. H. Schmehl, *Top. Curr. Chem.* **2007**, *281*, 101.
[18] a) N. M. Shavaleev, L. P. Moorcraft, S. J. A. Pope, Z. R. Bell, S. Faulkner, M. D. Ward, *Chem. Commun.* **2003**, 1134; b) N. M. Shavaleev, L. P. Moorcraft, S. J. A. Pope, Z. R. Bell, S. Faulkner, M. D. Ward, *Chem. Eur. J.* **2003**, *9*, 5283; c) N. M. Shavaleev, G. Accorsi, D. Virgili, Z. R. Bell, T. Lazarides, G. Calogero, N. Armaroli, M. D. Ward, *Inorg. Chem.* **2005**, *44*, 61; d) T. K. Ronson, T. Lazarides, H. Adams, S. J. A. Pope, D. Sykes, S. Faulkner, S. J. Coles, M. B. Hursthouse, W. Clegg, R. W. Harrington, M. D. Ward, *Chem. Eur. J.* **2006**, *12*, 9299; e) F. Kennedy, N. M. Shavaleev, T. Koullourou, Z. R. Bell, J. C. Jeffery, S. Faulkner, M. D. Ward, *Dalton Trans.* **2007**, 1492.
[19] S. Yajima, Y. Hasegawa, *Bull. Chem. Soc. Jpn* **1998**, *71*, 2825.
[20] F. Barigelletti, L. Flamigni, *Chem. Soc. Rev.* **2000**, *29*, 1.
[21] *Handbook of Photochemistry*, CRC Press, Boca Raton, FL, **2006**.
[22] a) S. I. Klink, L. Grave, D. N. Reinhoudt, F. C. J. M. van Veggel, M. H. V. Werts, F. A. J. Geurts, J. W. Hofstraat, *J. Phys. Chem. A* **2000**, *104*, 5457; b) G. A. Hebbink, D. N. Reinhoudt, F. C. J. M. van Veggel, *Eur. J. Org. Chem.* **2001**, 4101.
[23] N. M. Shavaleev, S. J. A. Pope, Z. R. Bell, S. Faulkner, M. D. Ward, *Dalton Trans.* **2003**, 808.
[24] J.-F. Wyart, A. Meftah, A. Bachelier, J. Sinzelle, W.-Ü L. Tchang-Brillet, N. Champion, N. Spector, J. Sugar, *J. Phys. B* **2006**, *39*, L77.
[25] a) B. Schlicke, P. Belser, L. De Cola, E. Sabbioni, V. Balzani, *J. Am. Chem. Soc.* **1999**, *121*, 4207; b) F. Barigelletti, L. Flamigni, M. Guardigli, A. Juris, M. Beley, S. Chodorowski-Kimmes, J.-P. Collin, J.-P. Sauvage, *Inorg. Chem.* **1996**, *35*, 136.
[26] G. M. Davies, S. J. A. Pope, H. Adams, S. Faulkner, M. D. Ward, *Inorg. Chem.* **2005**, *44*, 4656.
[27] S. G. Baca, S. J. A. Pope, H. Adams, M. D. Ward, *Inorg. Chem.* **2008**, *47*, 3736.
[28] S. Torelli, D. Imbert, M. Cantuel, G. Bernardinelli, S. Delahaye, A. Hauser, J.-C. G. Bünzli, C. Piguet, *Chem. Eur. J.* **2005**, *11*, 3228.
[29] J. N. Demas, G. A. Crosby, *J. Phys. Chem.* **1971**, *75*, 991.
[30] K. Nakamura, *Bull. Chem. Soc. Jpn.* **1982**, *55*, 2697.
[31] a) B. W. Van Der Meer, G. Coker III, S.-Y. S. Chen, *Resonance Energy Transfer: Theory and Data*, VCH Publishers, New York, **1994**; b) R. D. Jenkins, D. L. Andrews, *Photochem. Photobiol. Sci.* **2003**, *2*, 130.
[32] O. Bossart, L. De Cola, S. Welter, G. Calzaferri, *Chem. Eur. J.* **2004**, *10*, 5771.
[33] S. Welter, N. Salluce, A. Benetti, N. Rot, P. Belser, P. Sonar, A. C. Grimsdale, K. Müllen, M. Lutz, A. L. Spek, L. De Cola, *Inorg. Chem.* **2005**, *44*, 4706.
[34] A. I. Baba, W. Wang, W. Y. Kim, L. Strong, R. H. Schmehl, *Synth. Commun.* **1994**, *24*, 1029.
[35] a) R. Sahai, D. A. Baucom, D. P. Rillema, *Inorg. Chem.* **1986**, *25*, 3843; b) S. van Wallendael, D. P. Rillema, *Coord. Chem. Rev.* **1991**, *111*, 297; c) S. van Wallendael, M. W. Perkovic, D. P. Rillema, *Inorg. Chim. Acta* **1993**, *213*, 253.
[36] M. Furue, T. Yoshidzumi, S. Kinoshita, T. Kushida, S. Nozakura, M. Kamachi, *Bull. Chem. Soc. Jpn* **1991**, *64*, 1632.
[37] C. M. White, M. F. Gonzalez, D. A. Bardwell, L. H. Rees, J. C. Jeffery, M. D. Ward, N. Armaroli, G. Calogero, F. Barigelletti, *J. Chem. Soc. Dalton Trans.* **1997**, 727.
[38] B. P. Sullivan, D. J. Salmon, T. J. Meyer, *Inorg. Chem.* **1978**, *17*, 3334.
[39] M. J. Kendrick Geno, J. H. Dawson, *Inorg. Chim. Acta* **1985**, *97*, L41.
[40] a) M. F. Richardson, W. F. Wagner, D. E. Sands, *J. Inorg. Nucl. Chem.* **1968**, *30*, 1275; b) Y. Hasegawa, Y. Kimura, K. Murakoshi, Y. Wada, J. Kim, N. Nakashima, T. Yamanaka, S. Yanagida, *J. Phys. Chem.* **1996**, *100*, 10201.

Received: April 1, 2008
Revised: May 30, 2008
Published online: August 29, 2008

